River Flow 2010 - Dittrich, Koll, Aberle & Geisenhainer (eds) - © 2010 Bundesanstalt für Wasserbau ISBN 978-3-939230-00-7

Experimental analysis of the morphological evolution induced by a flow in a sudden channel constriction

L. Goutière & Y. Zech
Dept. of Civil Engineering, Université catholique de Louvain ; place du Levant, 1, B-1348 Louvain-la-Neuve, Belgium

C. Swartenbroekx & S. Soares-Frazão
Fonds National de la Recherche Scientifique and dept. of Civil Engineering, Université catholique de Louvain; place du Levant, 1, B-1348 Louvain-la-Neuve, Belgium

ABSTRACT: This paper presents an experimental study of a flow on movable bed in a channel featuring a sudden constriction. The experiments have been carried out at the Hydraulics Laboratory of the Université catholique de Louvain, Belgium. The experimental initial conditions consist of a flat and horizontal bed composed of uniform coarse sand. The boundary conditions are a steady flow without sediment supply upstream and a free outflow over a weir downstream. No sediment discharge is observed in the upstream wide part of the flume while significant morphological evolution of the bed is observed in the downstream narrow part. A scour hole forms at the corner of the constriction. This scour hole grows in time and the eroded sediments are transported further downstream. Part of these sediments deposes in the downstream part of the flume, generating a two-dimensional morphological evolution of the bed. To measure the evolution of the hydraulic and sedimentological parameters, different non-intrusive methods have been used and principally digital imaging techniques: interface detection for the bed level through the glass walls of the flume, particle tracking velocimetry for the water velocity at the flow free-surface and laser profile reconstruction for the bed morphological evolution at different times during the experiment. The analysis of these results allows to identify the different physical phenomena that govern the flow and its morphological evolution.

Keywords: Sudden constriction, Contraction, Narrowing, Morphology, Sediment transport, Digital imaging techniques, Topographical measurements

1 INTRODUCTION

Any sudden change in geometry in a canal or a river generally induces scouring that may be severe and damage the bank structures.

Scour has been largely studied through laboratory experiments in the context of bridge hydraulics (Hager 2008). Melville & Raudkivi (1977) described the flow occurring at the base of a cylindrical bridge pier within a scour hole. Capuano et al. (2004) analyzed the maximum scour depth around a rectangular abutment for small grain Reynolds numbers (between 5.3 and 9.0). Ettema & Muste (2004) studied the scale effects in small-scale model of flow around a spur dike over fixed bed. Sheppard & Miller (2006) tested local clear-water and live-bed pier scour with two different uniform cohesionless sediments. Kirkil et al. (2008) investigated coherent structures present in the flow field around a circular cylinder located in a scour hole. Nogueira et al. (2008) used Particle Image Velocimetry (PIV) to characterize the flow surrounding a cylindrical obstacle.

These experimental results are crucial to validate analytical and numerical models used for estimating the scour hole depth and the threshold value for scour entrainment or for simulating the temporal evolution of scour (Kothyari et al. 2007). For example, Richardson & Panchang (1998) compared Melville & Raudkivi (1977) observations with the simulations performed with a fully three-dimensional hydrodynamic model. Nagata et al. (2005) solved the fully three-dimensional Reynolds-averaged Navier–Stokes equation to calculate the flow field with water and bed surfaces varying in time around hydraulic structures and tested their model against laboratory data for spur dikes and bridge piers.

Scour is rather poorly documented in other context than bridge hydraulics. Dey & Raikar (2005) studied the effects of various parameters on scour depth in long constrictions for uniform

and non-uniform sediments under clear-water scour conditions. Palumbo et al. (2008) examined the impact of a sudden widening on a dam-break flow.

In this paper, the impact of a sudden constriction on a flow over a sand bed is investigated experimentally. The abrupt change of the flume width constitutes an obstacle to the flow. The contraction of the flow leads to clear-water scour. The morphological evolution of the channel bed and the flow characteristics were observed by non-intrusive measurement techniques.

2 EXPERIMENTAL SET-UP

Experiments of flow over a movable bed were carried out at the Hydraulics Laboratory of the Université catholique de Louvain, Belgium.

The tests were performed in a 7.4 m long flume, presenting on one side a sudden constriction, from 0.5 m to 0.3 m width, located 2 m upstream of the downstream end of the flume (Fig. 1). The constriction is realized in Perspex to allow to see and measure all the features that appear against the left side wall of the constricted part (Fig. 2). The sediment used is rather coarse sand with uniform grain-size distribution and a median diameter of 1.72 mm and relative density of 2.63, deposited with a porosity of 39 % (Becker & Kaiser 2008). The experimental initial condition is a flat sediment bed (Fig. 2) that is progressively saturated by introducing a small water discharge of 2 l/s at the upstream end. At this flow rate no sediment evolution is observed even in the narrow part of the flume. When the flat sediment bed is fully saturated, the upstream discharge is quasi-instantaneously increased to the regime value of 10 l/s. At this moment the water level increases rapidly to the regime level (approximately 120 s after the upstream discharge increase). The experiment is considered to start when the first grains move, which takes place at corner A of the constriction, approximately 20 s after the upstream discharge increase. The boundary conditions are a steady flow without sediment supply upstream and a free outflow over a weir downstream.

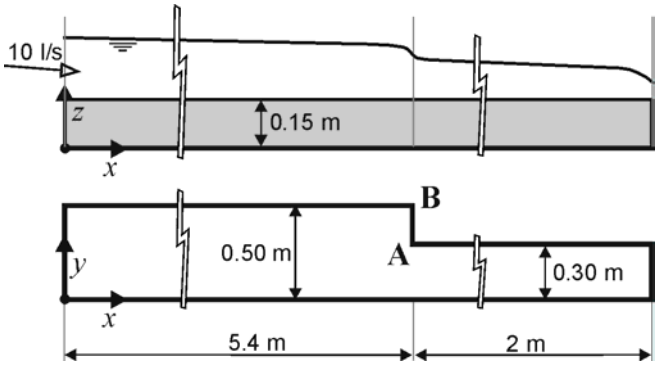

Figure 1. Experimental set-up: elevation view (top) and plane view (bottom).

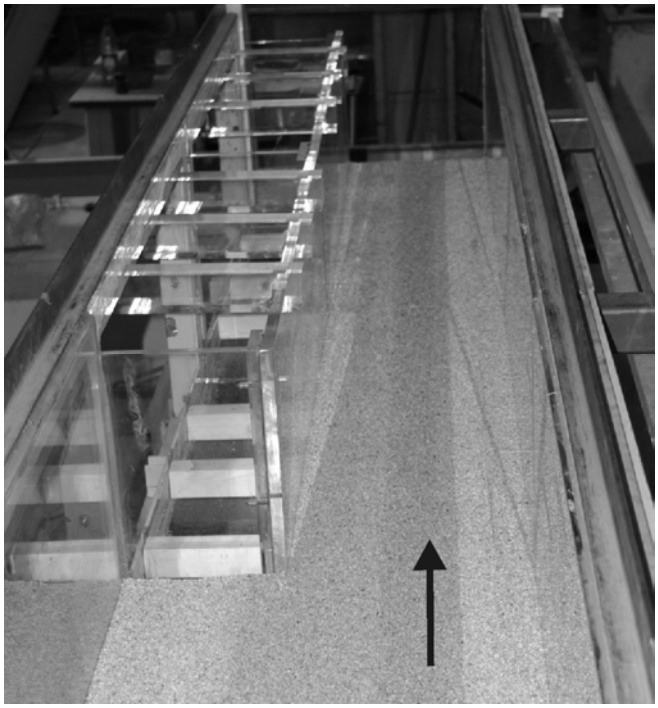
Figure 2. Experimental set-up: constriction with the initial flat sediment bed not yet saturated. Perspex structure used to realize the constriction.

3 FLOW DESCRIPTION

This section aims to describe the observed flow characteristics and the bed morphological evolution. An analysis of the observed features based on a literature review is carried out.

3.1 *Water profiles*

To have an idea of the expected water level, a one-dimensional computation was run, assuming a rigid bed. Regarding the horizontal initial bed slope and considering a global Manning roughness coefficient of 0.0167 s/m$^{1/3}$ for the whole channel, i.e. bed and side walls, the critical depth can be calculated along the whole flume (Fig. 3) while the uniform depth is equal to infinity. The critical depth presents a discontinuity at the beginning of the constriction due to the change in width. The downstream free outflow forces a

critical control section that imposes a critical downstream condition as end point of a subcritical water profile. The resulting flow is then subcritical over the whole channel. The water profile calculated by integration of the Bernoulli equation is represented in Figure 3. At the beginning of the constriction the water profile presents a lowering due to the flow acceleration in the contracted section, increasing the part of kinetic energy in the total available energy.

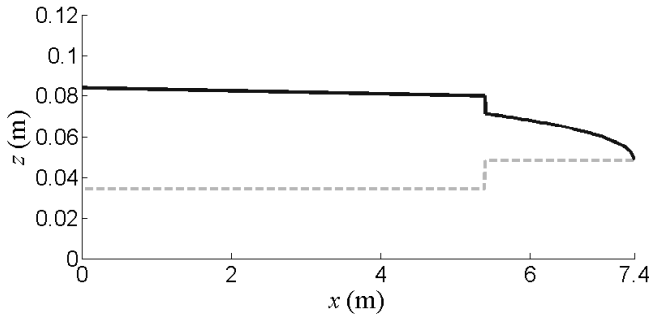

Figure 3. One-dimensional water profile: continuous line is the water level and dashed line the critical depth.

In the reality, the water profile is meanly the same as in one dimension but presents some variations in sections near and along the constriction. Just before the constriction, the water level is higher on left constricted side due to the reflection against the obstacle and the consequent velocity decrease, while velocity increases on the right side. This velocity dissymmetry propagates in the constriction entrance.

Finally, the sediment bed evolution induced by the variation of the hydraulic parameters along the *x*-axis and within cross-section progressively modifies the water profile in time.

3.2 *Morphological evolution*

The flow discharge has been chosen to generate sediment transport in the constriction reach only and not in the wider upstream reach. This particular situation allows to focus on the morphological evolution induced by a sudden discontinuity in the sediment transport capacity (Armanini & Di Silvio 1988), materialised by the change in this case from clear water flow to flow with bed-load transport. The increase of the sediment transport capacity in the constriction implies that the flow erodes sediments at the geometrical discontinuity located at the beginning of the constriction. Due to the three-dimensional downflow against the transversal wall and the increase of velocities at the constriction entrance (Breusers & Raudkivi 1991), the erosion generates a scour hole at its corner A (Fig. 4). Regarding the lack of sediment transport in the approaching flow, this erosion mechanism can be classified as a clear-water scour (Dey & Raikar 2005).

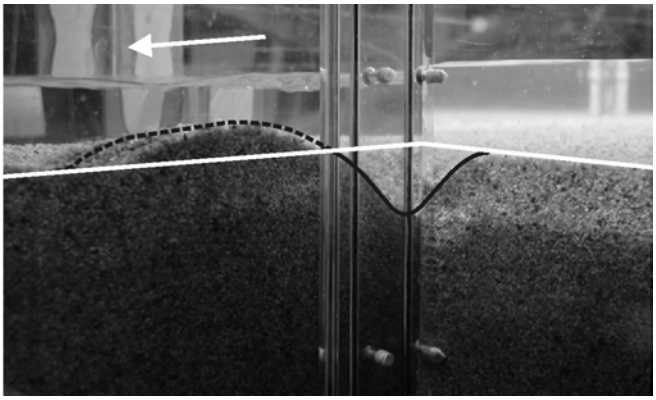

Figure 4. Creation of the scour hole located at corner A of the constriction: the white line is the initial bed level, the black continuous line marks the erosion scour hole and the black dashed line denotes the deposition crest.

The eroded sediments migrate in the constriction and generate a dissymmetrical evolution of the bed profile due to the two-dimensional flow. Indeed, the constriction of the fluid stream induces greater velocities on the right half of the channel than on the left (Fig. 5). It results that (i) on the left side, a part of the eroded sediments at corner A are deposited and generate a deposition crest (Fig. 4); (ii) on the right side, the main flow reaches its sediment transport capacity, carries further downstream the scoured sediments and erodes slightly the sediment bed.

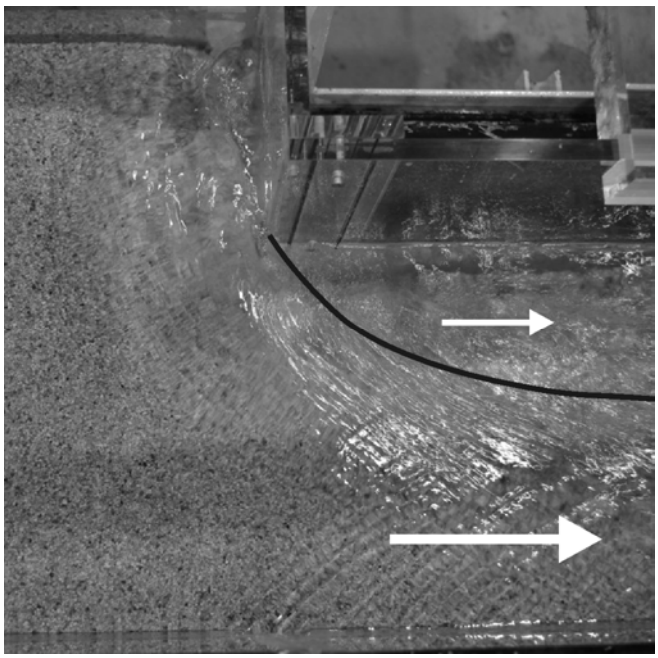

Figure 5. Flow constriction: greater velocities on the right side than on the left.

Progressively, the excess of sediment transported by the constricted flow velocity at the beginning of the constriction is deposited downstream in a way to reach the sediment transport capacity corresponding to a full-width flow recov-

ered after the constriction. The deposited sediments form an oblique front that migrates downstream until the end of the flume (Fig. 6).

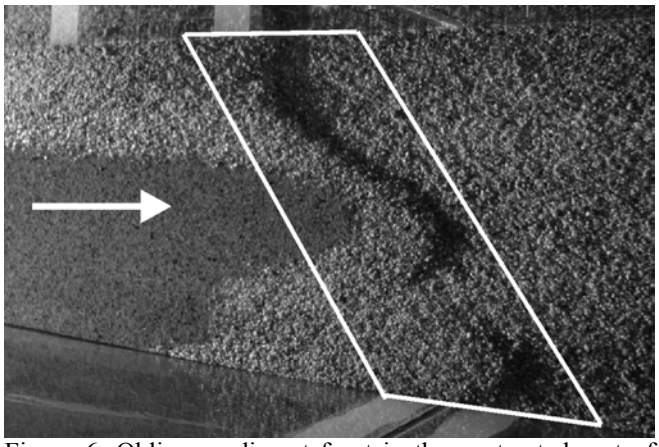

Figure 6. Oblique sediment front in the contracted part of the reach (picture taken after flume drying at the middle of the experiment).

The end of the experiment corresponds to the time when the scour hole has reached the left wall upstream of the constriction, which happens around 15 minutes after the beginning of the experiment. Indeed, at this moment, the erosion in the scour hole is not anymore sufficient to provide sediment corresponding to its transport capacity in the constriction and the flume bed empties progressively. The final shape of the scour hole after complete drainage of the water is shown in Figure 7. The upstream shape of the scour hole corresponds to a half ellipse whose centre is corner A of the constriction and major axis is transversal to the flow.

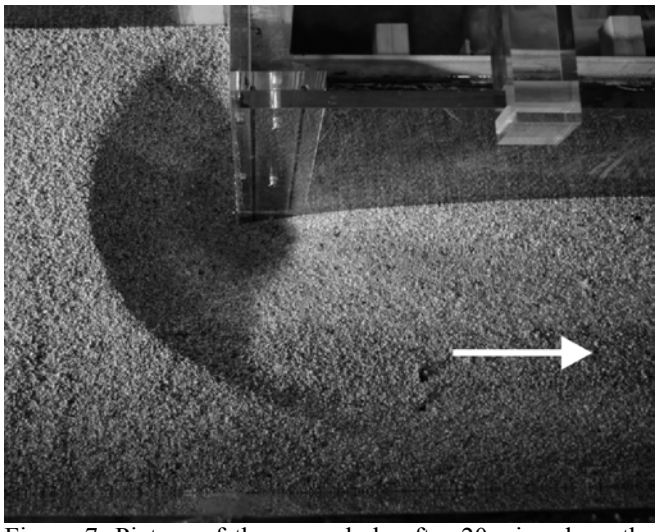

Figure 7. Picture of the scour hole after 20 min where the scour hole reaches the side walls.

4 EXPERIMENTAL MEASUREMENTS

The different measurement techniques used for this experiment are all non-intrusive and mainly based on digital imaging techniques. Some other measurement devices have been used in order to control the experimental conditions, to check locally the results obtained by image analysis and to provide directly important parameter evolution.

This section describes the different measurements techniques and the main obtained results, in order to quantify the water and morphological characteristics, qualitatively described in former section.

4.1 *Water levels*

The evolution in time of the water level is provided by four ultrasonic gauges, one located in the upstream part of the wide reach unaffected by the flow contraction and three located around the constriction corner, as sketched in Figure 8. All the gauges are located 0.15 m away from the flume walls and at minimum 0.2 m from each other in order to avoid parasitic reflections of the ultrasonic waves.

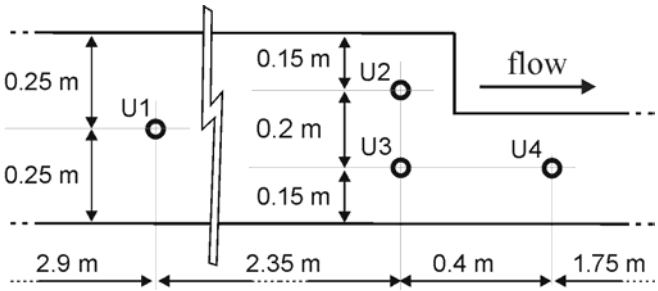

Figure 8. Position of the four ultrasonic gauges.

These measurements give the evolution of the water level and also allow to check the repeatability of the experiment. Indeed, initial and boundary conditions being very sensitive, it is essential to check that the different experimental runs can be combined to form one single data set. This repeatability is assumed as satisfactory if the measured water levels from different runs are in good agreement.

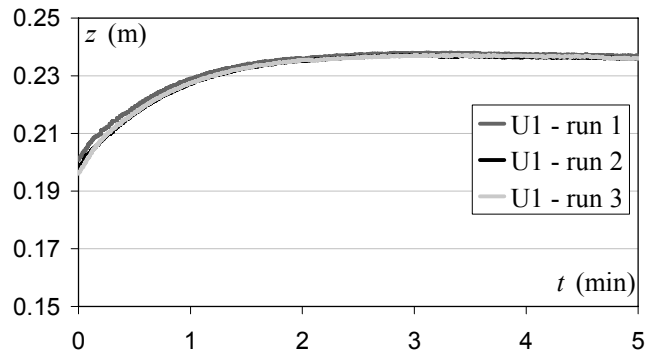

Figure 9. Repeatability check of experimental conditions with gauge U1.

As an example, Figure 9, showing the measured water level at gauges U1 for three different

runs, confirms that the flow is identical between three different runs.

Figure 10 shows the water level evolution for three ultrasonic probes, U2, U3 and U4. The ultrasonic probe U2 presents some erratic signals but the actual level evolution is easy to deduce from the raw data. The three sets of water level illustrated in the figure are coherent with the known hydraulic features of a flow in a constriction. Indeed, as explained in Section 3.1: (i) before the constriction, the level of the narrowed side (left side, U2) is higher than the level on the other side (right side, U3); (ii) after the constriction, the level is lower than before (U4).

These results evidence the required time to reach the flow regime condition. The water level increases during approximately 120 s before becoming stable, but 80 % of the evolution between initial and regime levels are reached in 60 s.

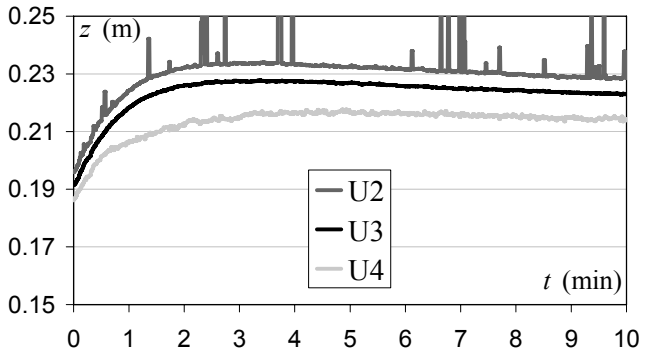

Figure 10. Water level evolution at gauge U2, U3 and U4.

4.2 *Surface velocities*

The surface velocities are calculated by particle tracking velocimetry (PTV) algorithms in two dimensions (Capart et al. 2002). Pictures of floating tracers spread on the water surface are taken from above of the flume at a frequency of fifteen frames per second in order to reconstruct the trajectories of the different tracers. For these experiments the flow has been filmed with 4 different positions of the camera: every 0.7 m from 0.8 m before the constriction ($x = 4.6$ m) to the downstream end of the flume ($x = 7.4$ m). An additional acquisition window has been taken around the constriction corner, between $x = 5.1$ m and $x = 5.7$ m. From the trajectories of each particle at the water surface, the velocities are easily derived.

Figure 11 shows the tracer trajectories around the constriction at time $t = 3$ minutes. The picture is constructed from ten successive images and is similar to a long-exposure photograph. The constriction of the flow is clearly observable.

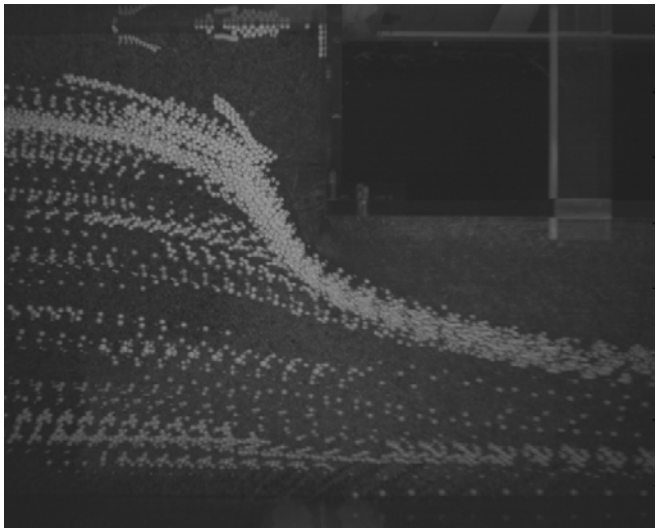
Figure 11. Artificial long exposition of the camera sensor over a range of ten frames around 3 minutes after the beginning of the experiment.

Figure 12 shows the velocities on a structured grid around the constriction at time $t = 3$ minutes, corresponding to the tracer positions given in Figure 11. The velocities are calculated by averaging the particle velocities in grid cells of 2.5 cm by 2.5 cm during ten successive images, i.e. during 0.667 s. The velocity increase in the constriction is clearly observable. The average cross section velocities goes, approximately, from 0.3 m/s before the constriction to 0.7 m/s after.

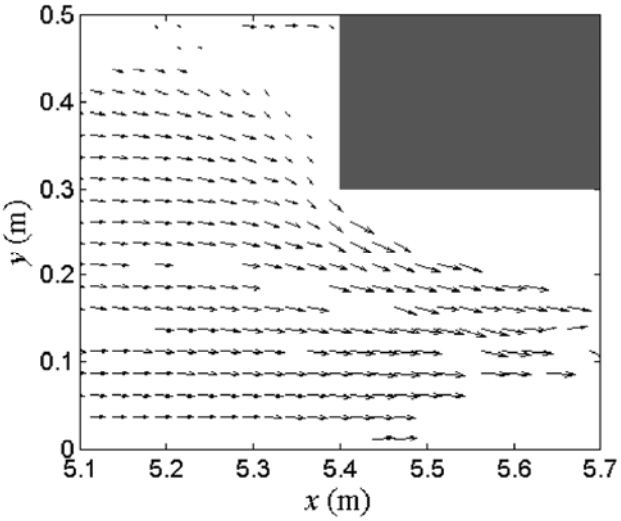

Figure 12. Velocity field around the constriction corner at time $t = 3$ minutes.

4.3 *Sediment bed level evolution*

The transparent side walls of the constriction allow to observe the bed level evolution against these side walls. As the maximum erosion and deposition rates appear against these walls, the automatic detection of the interface between sediment and water is easy to produce by illuminating the back of the picture, in this case the right side of the flow (Fig. 13). The detection is real-

ized by finding the maximum of light intensity gradient on pictures. Pictures have been taken every ten seconds until fifteen minutes after the experiment beginning.

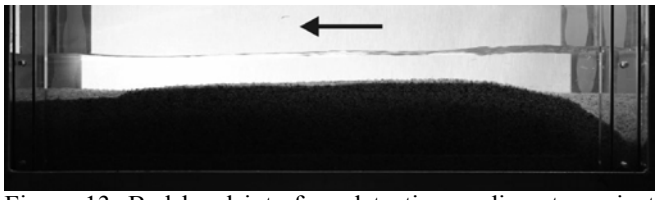

Figure 13. Bed level interface detection, sediments against the left constriction side wall are the darker area.

The sediment bed level evolution is given along the two walls forming the corner of the constriction, Figure 14 depicts the bed along the transversal front wall of the constriction and Figure 15 features the first meter of the left side wall after the constriction. The levels are given at time t = 1, 2, 3, 5, 7 and 10 minutes, respectively.

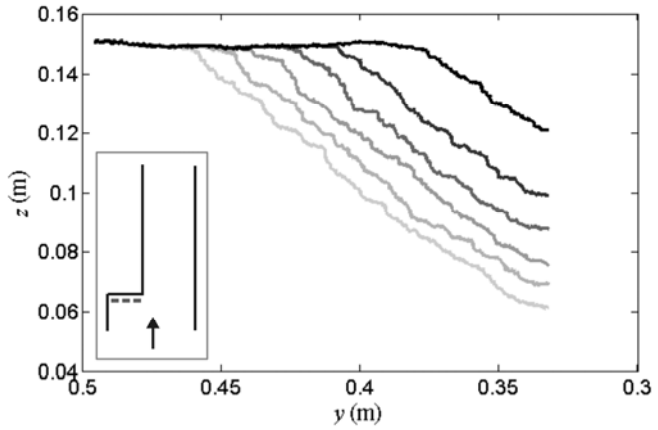

Figure 14. Sediment level evolution against the transversal front wall of the constriction at time, t = 1, 2, 3, 5, 7 and 10 minutes, from darker to brighter.

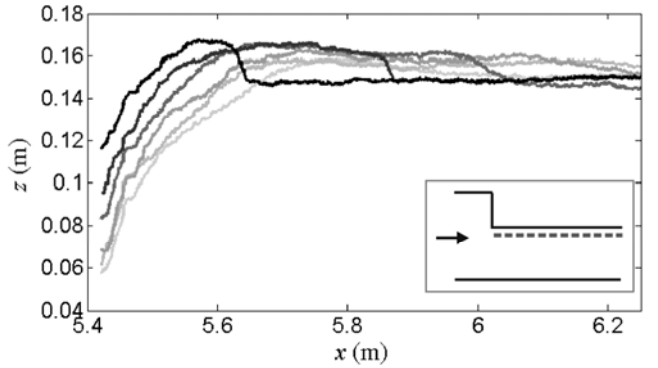

Figure 15. Sediment level evolution against the left side wall of the constriction at time, t = 1, 2, 3, 5, 7 and 10 minutes, from darker to brighter.

These results highlight the evolution of the scour hole and the deposition crest. The deposition crest reaches is maximum level in the first minute and progressively decreases in height while spreading downstream. The scour hole forms quickly, the half major axis is about 8 cm and the depth is about 3 cm in one minute, and progressively becomes deeper and wider. The hole deepening and widening is decelerated with time. The slope along the major axis of the elliptical scour hole is constant in time and is equal approximately to 32°, giving an idea of the submerged angle of stability of the sand.

4.4 *Bed topography*

The morphological changes generated by the flow were measured at different times during the experiment. A laser sheet imaging technique, described in more details in Soares-Frazão et al. (2007), has been used to measure the shape of successive cross-sections before and in the constriction. The measurement technique consists in taking pictures of the bed profile with a digital camera while a laser-sheet lights up a particular cross-section. A preliminary calibration procedure defines an affine transformation which allows to convert the pixel coordinates of the laser profile on the 2D camera image into 3D metric coordinates.

In order to reconstruct the entire bed topography, the acquisition devices (camera and laser) are fixed on a moving system along x-axis, that allow to take picture of each desired cross-section in the same configuration, and then with the same calibration (Fig. 16). During each topographical survey, the flow is stopped and the water drained off in order to take the pictures on a dry sediment bed.

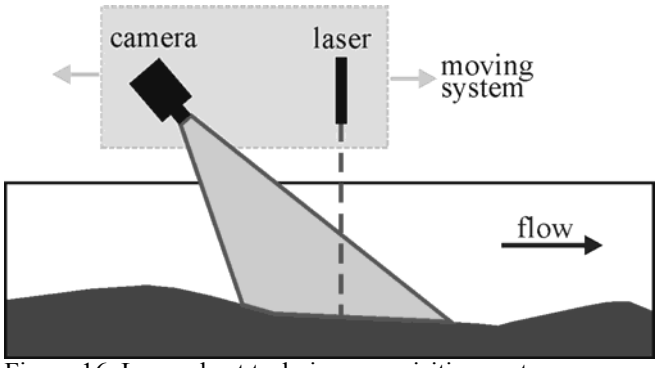

Figure 16. Laser-sheet technique acquisition system.

In the present case, the analysed sections are located every 1 cm from 5.25 m to 5.55 m, around the constriction beginning, and every 5 cm from 5.55 m to 7.35 m.

Figure 17 gives the reconstructed topography at three different times. All figures illustrate clearly the scour hole located at the corner of the constriction (x = 5.4 m and y = 0.3 m), the deposition crest (5.6 < x < 6.2 m and y ~ 0.25 m) and the oblique sediment front. As shown in Figure 18, the scour hole presents a half elliptic shape upstream of the constriction, as already explained in Section 3.2.

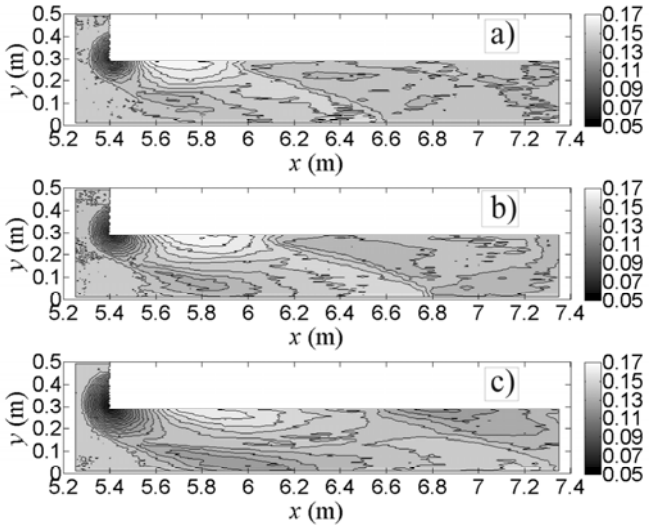

Figure 17. Bed topography of the downstream end of the channel at different times (levels in m): a) t = 3 min, b) t = 5 min and c) t = 7 min.

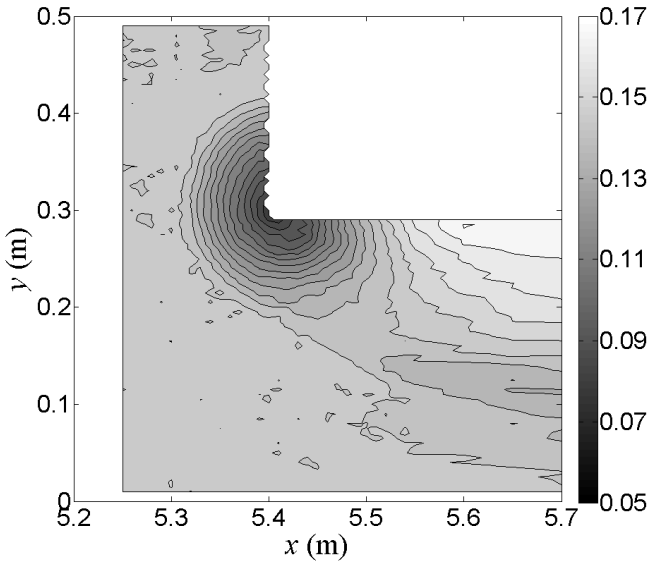

Figure 18. Zoom on the scour hole at times t = 7 min (levels in m).

4.5 *Manual measurements*

Some manual punctual measurements have been made during the experiments. These additional data are useful to have direct and accurate information on important parameters but also to validate the other measurement techniques.

These measurements focus on the scour hole size and shape (distances a, b and c in Fig. 19), the sediment level z_s at centre of the scour hole and the bed load sediment volume carried out of the flume ($V_{sb,out}$ in Fig. 19).

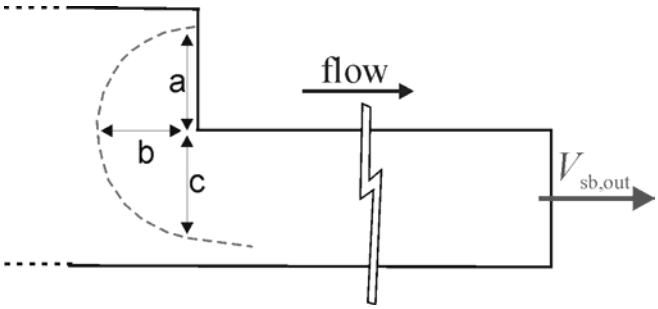

Figure 19. Manual measurements.

Figure 20 shows the evolution of parameters a, b, c and z_s, and confirm that the scour hole presents a half elliptic shape as a and c are practically equal and greater than b. The evolution of these parameters is rather fast in the first stages of the experiment, from 0 to 3 s, then slows down afterwards. The sediment level at the scour hole centre z_s presents the same evolution in time and tends to a minimum equal to 0.04 m. The manual measurements of the scour hole size are in good agreement with digital imagery measurements. Moreover, the resulting evolution in time of the scour depth is in agreement with the asymptotical scour depth evolution due to bridges piers in case of clear-water scour, related in Raudkivi (1990).

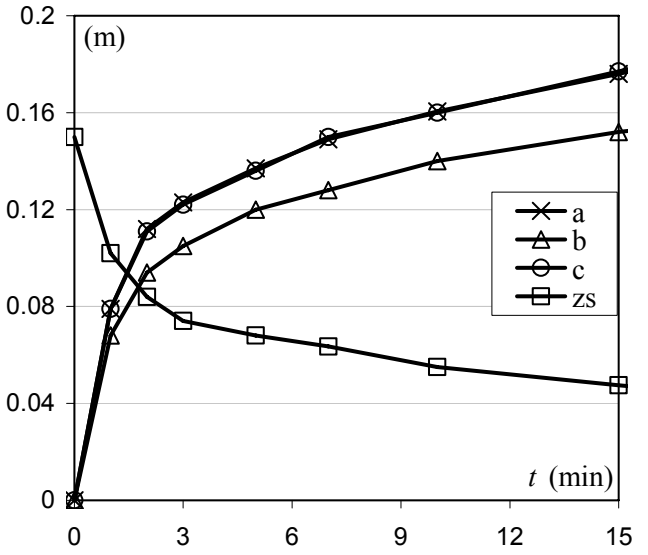

Figure 20. Evolution in time of scour hole shape parameters a, b, c and sediment level at the scour hole centre z_s.

The sediments transported out of the flume are collected and weighted after drying. Regarding the grain specific weight and the porosity of the sediments, in this case equals to 25.8 kN/m³ and 0.39 respectively, the sediment volume $V_{sb,out}$ can be calculated. The time evolution of this volume is represented in Figure 21. It is quasi linear between 2 and 10 min, but again greater in the first stage of the experiment. This linear evolution corresponds to a constant sediment outflow that seems consistent with the observed flow stabilisation that progressively appears in the experiment.

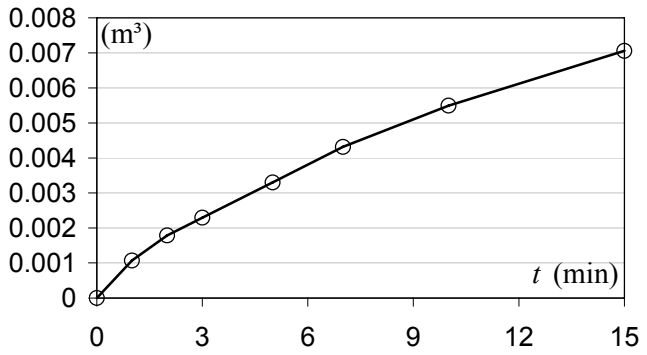

Figure 21. Sediment volume carried out of the flume $V_{sb,out.}$

5 CONCLUSION

This paper presents the experiments of a clear-water scour generated by a sudden constriction.

The flow is qualitatively described from experimental observation and compared to previous analyses found in literature but generally developed for scouring around bridge piers and abutments.

The implemented non-intrusive measurement techniques allow to quantify the water level and velocities and also the morphological evolution of the bed, along the side walls and over the whole flume.

The main observations concern the formation of the scour hole located at the constriction corner. It presents an asymptotical evolution in time and features an elliptical shape. The evolution of the sediment bed in the constriction is two-dimensional due to the flow pattern. These results match particularly well the literature devoted to bridge piers and abutments.

REFERENCES

Armanini, A., and Di Silvio, G. 1988. A one-dimensional model for the transport of a sediment mixture in non-equilibrium conditions. Journal of Hydraulic Research, 26(3), 275-292.

Becker, A. and Kaiser, D. 2008. Ecoulement consecutif à une rupture de barrage dans un canal présentant un élargissement brusque: mesures de la surface libre et de la topographie finale (in French). MSc thesis, Université catholique de Louvain, Louvain-la-Neuve, Belgium.

Breusers, H.N.C., and Raudkivi, A.J. 1991. Scouring. Hydraulic structures design manual 2, IAHR, A.A. Balkema, Rotterdam, The Netherlands.

Capart, H., Young, D.L., and Zech, Y. 2002. Voronoï imaging methods for the measurement of granular flows. Experiments in Fluid, 32, 121-135.

Capuano, D., Carravetta, and A., Golia, U.M. 2004. Activation of scour around bridge abutment. Proc. of River Flow 2004, Greco, M. et al. (eds.), Naples, Italy, 563-568.

Dey, S., and Raikar, R.V. 2005. Scour in long contractions. Journal of Hydraulic Engineering, 131(12), 1036-1049.

Ettema, R., and Muste, M. 2004. Scale effects in flume experiments on flow around a spur dike in flatbed channel. Journal of Hydraulic Engineering, 130(7), 635-646.

Hager, W.H. 2008. Advances in scour hydraulics. Proc. of River Flow 2008, Altinakar, M. et al. (eds.), Çeşme, Turkey, 23-42.

Kirkil, G., Constantinescu, S.G., and Ettema, R. 2008. Coherent structures in the flow field around a circular cylinder with scour hole. Journal of Hydraulic Engineering, 134(5), 572-587.

Kothyari, U., Hager, W., and Oliveto, G. 2007. Generalized approach for clear-water scour at bridge foundation elements. Journal of hydraulic Engineering, 133(11), 1229-1240.

Melville, B.W., and Raudkivi, A.J. 1977. Flow characteristics in local scour at bridge piers. Journal of Hydraulic Research, 15(4), 373–380.

Nagata, N., Hosoda, T., Nakato, T., and Muramoto, Y. 2005. Three-dimensional numerical model for flow and bed deformation around river hydraulic structures. Journal of Hydraulic Engineering, 131(12), 1074-1087.

Nogueira, H.I.S., Franca, M.J., Adduce, C., and Ferreira, R.M.L. 2008. Bridge piers in mobile beds: visualization and characterization of the surrounding and approaching flows. Proc. of River Flow 2008, Altinakar, M. et al. (eds.), Çeşme, Turkey, 2397-2406.

Palumbo, A., Soares-Frazão, S., Goutière, L., Pianese, D., and Zech, Y. 2008. Dam-break flow on mobile bed in a channel with a sudden enlargement. Proc. of River Flow 2008, Altinakar, M. et al. (eds.), Çeşme, Turkey, 645-654.

Raudkivi, A. 1990. Loose Boundary Hydraulics, 3rd edition. Pergamon Press, Oxford, UK.

Richardson, J.E., and Panchang, V.G. 1998. Three-dimensional simulation of scour-inducing flow at bridge piers. Journal of Hydraulic Engineering, 124(5), 530–540.

Sheppard, D.M., and Miller, W. 2006. Live-bed local pier scour experiments. Journal of Hydraulic Engineering. 132(7), 635-642.

Soares-Frazão, S., le Grelle, N., Spinewine, B., and Zech, Y. 2007. Dam-break induced morphological changes in a channel with uniform sediments: measurements by a laser-sheet imaging technique. Journal of Hydraulic Research, 45 Extra Issue, 87-95.